Diels–Alder Exo Selectivity in Terminal-Substituted Dienes and Dienophiles: Experimental Discoveries and Computational Explanations

6 AUTHORS, INCLUDING:

Yu-hong Lam
University of California, Los Angeles
15 PUBLICATIONS 221 CITATIONS

SEE PROFILE

Paul Ha-Yeon Cheong
Oregon State University
45 PUBLICATIONS 2,036 CITATIONS

SEE PROFILE

Jose Blasco
PharmaMar
1 PUBLICATION 49 CITATIONS

SEE PROFILE

Véronique Gouverneur
University of Oxford
179 PUBLICATIONS 4,869 CITATIONS

SEE PROFILE

Diels–Alder *Exo*-Selectivity in Terminal-Substituted Dienes and Dienophiles: Experimental Discoveries and Computational Explanations

Yu-hong Lam[†], **Paul Ha-Yeon Cheong**[‡], **José M. Blasco Mata**[†], **Steven J. Stanway**[§], **Véronique Gouverneur**[†], and **K. N. Houk**[‡]
Chemistry Research Laboratory, University of Oxford, UK; Department of Chemistry and Biochemistry, University of California, Los Angeles, CA 90095; Neurology and GI Centre of Excellence for Drug Discovery, GlaxoSmithKline, Harlow, Essex, UK

Abstract

The Diels–Alder reactions of a series of silyloxydienes and silylated dienes with acyclic α,β-unsaturated ketones and N-acyloxazolidinones have been investigated. The *endo*/*exo* stereochemical outcome is strongly influenced by the substitution pattern of the reactants. High *exo* selectivity was observed when the termini of the diene and the dienophile involved in the shorter forming bond are both substituted, while the normal *endo* preference was found otherwise. The *exo*-selective asymmetric Diels–Alder reactions using Evans' oxazolidinone chiral auxiliary furnished a high level of π-facial selectivity in the same sense as their well-documented *endo*-selective counterparts. Computational results of these Diels–Alder reactions were consistent with the experimental *endo*/*exo* selectivity in most cases. A twist-asynchronous model accounts for the geometries and energies of the computed transition structures.

Introduction

Precise control of stereoselectivity in the installation of asymmetric centers constitutes a prominent goal in organic synthesis. The Diels–Alder reaction is indispensable for the stereoselective construction of six-membered rings,[1] a structural motif widely found in natural products. In its intermolecular variant, a cyclohexene ring with up to 4 stereocenters can be formed in a single step from acyclic precursors, often with high levels of regio- and stereocontrol. A familiar property of this reaction, whether thermal or catalyzed, is the *endo* diastereoselectivity.[2] As a result, the formation of these stereogenic centers on the ring is often regarded as "predictable in a relative sense."[3]

In contrast, instances of the Diels–Alder reaction showing *exo*-selectivity occur less frequently, at least in an intermolecular context. Apart from some isolated cases,[4, 5] certain structural motifs on the dienophile are well-known to lead predominantly to *exo* cycloadducts, including conformationally restricted cyclic s-*cis*- dienophiles,[6] and α-halo α,β-unsaturated carbonyl compounds.[7]

veronique.gouverneur@chem.ox.ac.uk; houk@chem.ucla.edu.
[†]University of Oxford.
[‡]University of California, Los Angeles.
[§]GlaxoSmithKline.

Synthetic protocols geared toward an *exo*-selective Diels–Alder reaction usually entail the use of structurally elaborate starting materials that incorporate strategic design features. These features are often anticipated to sterically encumber the *endo* mode of approach of the reactants. (Scheme 1) Danishefsky has utilized a *gem*-dimethyl group and a bulky aroyl group on the diene and dienophile respectively to divert the cycloaddition into the desired *exo* manifold by virtue of their steric bulk. This was applied in the total synthesis of racemic mamanuthaquinone. [8] (Eq. 1)

Homochiral α,β-unsaturated *N*-acylamino Fischer carbenes containing an oxazolidinone or imidazolidinone moiety have been used as *exo*-selective dienophiles in cycloadditions of cyclopentadiene and other acyclic dienes.[9] The apically disposed carbonyl ligands on the octahedrally coordinated metal center furnished the steric hindrance for impeding the *endo* trajectory. (Eq. 2) Other stoichiometric organometallic reagents have also been reported to give a high *exo* selectivity.[10]

An early example of catalyst-controlled *exo*-selective Diels–Alder reactions was reported by Yamamoto et al. The bulky Lewis acid, aluminum tris(2,6-diphenylphenoxide), was shown to facilitate *exo* cycloaddition of cyclopentadiene and phenyl vinyl ketone, a pair of reactants which give predominantly an *endo* cycloadduct otherwise.[11] (Eq. 3) *Exo*-selective cycloadditions of cyclopentadiene or diphenylisobenzofuran and α,β-unsaturated aldehydes have been documented by MacMillan amongst the first highly enantioselective organocatalytic Diels–Alder reactions.[12] More recently, Ishihara *et al.* reported the use of a chiral binaphthyl-substituted diamine in cycloadditions using α-acyloxyacroleins as dienophiles.[13] A structurally related, binaphthyl-based diamine was found by Maruoka to be an effective catalyst in the *exo*-selective cycloadditions with *trans*-cinnamaldehyde and two other α,β-unsaturated aldehydes.[14] The high *exo* selectivity has been attributed to the steric hindrance of the binaphthyl moiety in the reactive iminium intermediate formed from the dienophile and the catalyst.[15] (Eq. 4) Hayashi extended the scope of α,β-unsaturated aldehydes suitable for *exo*-selective cycloadditions by using a diarylprolinol silyl ether as the organocatalyst.[16] In all these reports on organocatalyzed Diels–Alder reactions, instances where a high *exo*-selectivity is observed involve the use of cyclopentadiene as the diene component.

Examples of *exo*-selective Diels–Alder reactions are also found in host-guest chemistry. Thus, a trimeric porphyrin host facilitates an exclusively *exo* cycloaddition of a furan and a maleimide by orienting them in the required disposition.[17] The *exo* orientation can also be fulfilled by hydrogen bonding within the supramolecular complex.[18] Monoclonal antibodies that catalyze enantioselective Diels–Alder reactions of *N*-acylamino-1,3-butadienes and *N,N*-dimethylacrylamide in an either *endo*- or *exo*-specific fashion have also been derived.[19]

During the study of the preparation of enantioenriched fluorinated carbocycles,[20] we synthesized an array of Diels–Alder cycloadducts featuring an allylsilane or a silyl enol ether, starting respectively from all-carbon silylated dienes[21] or silyloxy dienes.[22, 23] (Scheme 2) We have observed a remarkable change in the *endo/exo* stereoselectivity of the cycloaddition that depends on the substitution pattern of the starting material. As depicted in Scheme 2, when both R_1 and R_2 groups are a methyl group (right, Scheme 2), the adducts with four stereocenters are formed with a consistently high *exo* selectivity. Use of the desmethyl diene and/or dienophile leads to the "normal" *endo* products predominantly (left, Scheme 2). The observation that such a minor modification of substituents on these common substrates could lead to a dramatic change in *endo/exo* selectivity is intriguing, not least because it holds obvious implications in the stereodefined synthesis of carbocycles in general. We now detail the synthetic results obtained with this class of substituent-dependent, *exo*-selective Diels–Alder reactions, as well as computational studies that reveal the origins of these selectivities.

Synthetic Results and Discussion

The dienes **1**−**2** and dienophiles **3**−**6** that form the basis of this work are shown in Chart 1. The silylated and silyloxydienes,[24] and the dienophiles[25] were either readily synthesized by reported methods or were commercially available.

The Diels–Alder reactions involving the α,β-unsaturated N-acyloxazolidinone **3** and their asymmetric variant mediated by Evans' chiral auxiliary **3***[26] are listed in Entries 1−8 of Table 1. These were performed in dichloromethane at −40 °C promoted by 1.4 equivalents of Me$_2$AlCl. As previously reported,[20] the asymmetric Diels–Alder reaction of silylated diene **1a** with the homochiral **3*** delivered *endo*-**7** as the major product with complete C$_\alpha$-*Re* facial selectivity.[26] (Entry 1) Under otherwise identical conditions, however, diene **1b**, which has an extra C1-methyl group, afforded *exo*-**8** as the sole isolated product. (Entry 2) As proved by X-ray crystallography of *exo*-**8**, this cycloaddition also arises from the attack on the homochiral dienophile from its C$_\alpha$-*Re* face exclusively. The sense of asymmetric induction in this case is thus identical to that observed in their *endo*-selective counterparts involving **1a** and other reported dienes.[26] Reaction of diene **1c** bearing an additional methyl group at C3 yielded comparable results. (Entry 3) The sense of asymmetric induction in both *endo*- and *exo*-selective cycloadditions could be explained by Evans' model.[26] (Figure 2) The oxazolidinone–Lewis acid complex is rigidified by chelation of both carbonyl groups to the aluminum. The benzyl group of the chiral auxiliary effectively shields the C$_\alpha$-*Si* face of the dienophile, giving rise to the sense of facial selectivity observed.

The same substituent-dependent variation in *endo*/*exo* selectivity was observed in the Diels–Alder reactions of 2-silyloxy-1,3-butadienes with **3** and **4**. Thus the cycloaddition of diene **2a** and the achiral acryloyl oxazolidinone **4** was highly *endo* selective, (Entry 4) while the same reaction with the crotonyl oxazolidinone **3** gave the *exo* cycloadduct **11** as the only product. (Entry 5) The stereoselectivity was not affected to any appreciable extent by changing either the silyl protecting group or the C4 substituent of the diene. The TIPS-protected silyloxydiene **2b** and the 1,4-dimethyl silyloxydiene **2c** delivered respectively *exo*-**12** (Entry 6) and *exo*-**13** (Entry 7) highly selectively upon cycloaddition with **3**. The asymmetric cycloaddition of the silyloxydiene **2d** with **3*** also yielded the expected product *exo*-**14** in high *exo*/*endo* and facial selectivities. (Entry 8) The high *exo*-selectivity of asymmetric carbo Diels–Alder reactions using the auxiliary of **3*** is rare in an intermolecular context.[27]

α,β-Unsaturated ketones have also been studied with silylated or silyloxy dienes in the presence of catalytic Me$_2$AlCl. (Entries 9−11) The same trend in *endo*/*exo* selectivity with substitution pattern was found. Thus predominantly *endo* cycloaddition occurred when either C1 of the diene (Entry 9) or the β-position of the dienophile (Entry 10) was unsubstituted. For the combination of diene **1b** and dienophile **5**, each of which contained a terminal methyl group on the reacting double bonds, the reaction was *exo*-selective. (Entry 11)

The stereochemistry of the cycloadducts was readily assigned for all cycloadducts based on proton NMR coupling constants (Figure 3), and confirmed in the case of *exo*-**8** by X-ray crystallography. In the *exo* cycloadducts, the signal due to the methine ring proton (H1, See Figure 1 for numbering) geminal to the carbonyl group appears as a triplet of ca. 10 Hz, consistent with vicinal coupling of H1 to two *trans*-diaxial protons (H2 and H6). In the *endo* counterparts with a C6-Me group (*endo*-**7**[20] and **15**), this signal exists as a doublet of doublets with coupling constants of about 10 and 6 Hz, which arise, respectively, from one *trans*-diaxial and one axial-equatorial pair of coupling spins. The couplings of H1 in cycloadducts derived from acryloyl dienophiles (*endo*-**10** and **16**) were also consistent with their stereochemistry.

Acyclic 2-silyloxy-1,3-butadienes substituted at one or both termini are useful dienes in Diels–Alder reactions toward a number of medicinally relevant targets. Despite their structural

simplicity, the stereochemical outcome observed with these substrates and cyclic dienophiles proves to be subtly dependent on the structure of the reactants and the Lewis acid.[22, 28] The variation of the observed *endo/exo* selectivity with substitution pattern was rationalized in terms of steric clash between substituents attached on the approaching diene and dienophile. On the other hand, the use of oxazolidinone-containing dienophiles of the type **3*** in R_2AlCl-mediated Diels–Alder reactions is well precedented for simple dienes, and the use of 2-silyloxydienes was documented recently.[29] We computationally investigated the TSs of the current series of cycloadditions, focusing on how the substitution pattern of the starting material impacts on the stereochemical outcome.

Computational Methodology

Geometry optimization and thermodynamic corrections were performed with hybrid density functional theory (B3LYP)[30] using the 6−31G(d)[31] basis set. MP2 (default, frozen core)/6−31+G(d)//B3LYP/6−31G(d) single-point energies of *endo* and *exo* transition states have also been computed and compared with the B3LYP derived values and experimental data where available. Solvation corrections for the experimentally used solvent, dichloromethane, were calculated by the PCM method[32] and UAKS radii with single-points at the HF/6−31+G(d,p) level of theory.[33]

Optimization of transition structure geometries was started from a boat-like input structure expected from the general Diels–Alder reaction. The distance of the shorter forming bond (C5–C6) was first held fixed and the remainder of the structure optimized. This distance constraint was then lifted, and the structure was re-optimized to the transition state.[34] All energy minima and transition structures were characterized by frequency analysis.

All calculations were performed with *Gaussian 03*.[35]

Computational Results and Discussion

We first computationally examined a Diels–Alder reaction with the oxazolidinone-containing dienophile **3** for which experimental data were available. Dienophile **3** in the presence of Me_2AlCl was represented by the bidentate complex **A₂** in computations. (Figure 4) Chiral complexes of the type **A₂** have been invoked as the reactive species in R_2AlCl-mediated asymmetric Diels–Alder reactions,[26] and have been characterized in solution by NMR.[36]

The Me_2AlCl-mediated cycloaddition of silyloxydiene **2c** and **3** was completely *exo*-selective. (Table 1, Entry 7) The *endo* and *exo* TSs of the **2c**+**A₂** addition are presented showing their boat-like geometries in Figure 4. B3LYP and MP2 predict a difference in electronic activation barrier of 2.9 and 2.1 kcal/mol, respectively, both in favor of the *exo* pathway (See Table 2 below). The difference in free energy of activation between the *endo* and the *exo* approaches, after correcting for solvent effects, is 4.0 kcal/mol. (Figure 4) The experimental level and sense of diastereoselectivity was thus consistent with computation. The activation enthalpies refer to the difference between the enthalpy of the TS and the sum of enthalpies of diene and the dienophile complex infinitely separated in the gas phase. The small and negative gas-phase $\Delta H^{\ddagger}$ (and the negative $\Delta E^{\ddagger}$, see below) values are often observed in modeling gas-phase ion/molecule reactions in general.[37, 38] In the present case they are consistent with the more favorable electrostatic attractions expected between the diene's electrons and the cationic **A₂** at the TS, compared with the separate, unbound state.

Decomposition of the activation barrier ($\Delta E^{\ddagger}$) into distortion ($\Delta E_d^{\ddagger}$) and interaction energies ($\Delta E_i^{\ddagger}$)[37, 39] yields valuable insight into the differing activation energies of the *endo* and *exo* pathways. This analysis has previously been applied in understanding 1,3-dipolar and Diels–Alder cycloadditions.[40] The distortion energy is the energy required to distort the diene and

the dienophile complex into the geometries they have at the transition state without allowing interaction between them. The activation barrier is then the sum of distortion and interaction energies: $\Delta E^{\ddagger} = \Delta E_{\mathrm{d}}^{\ddagger} + \Delta E_{\mathrm{i}}^{\ddagger}$, where the interaction energy term encompasses all the stabilizing and repulsive interactions between the diene and dienophile fragments at the transition state. Table 2 lists the activation, transition-state distortion and transition-state interaction energies for the *endo* and *exo* Diels–Alder TSs of **2c**+**A$_2$**, computed by B3LYP and MP2 methods.

The distortion energy values calculated by either B3LYP or MP2 are very similar in most cases, but MP2 predicts that the interactions at the *endo* TS are more stabilizing than the *exo* by a larger margin than B3LYP does. MP2 favors the *endo* pathway to a greater extent than B3LYP for all cycloadditions. The underestimation of *endo/exo* selectivity by B3LYP due to problems in describing long-range dispersion interactions has been noted.[41, 42]

It is noteworthy that the interactions between the diene and dienophile fragments are more stabilizing at the *endo* TS than at the *exo* TS, regardless of the computational method used. The net preference of *exo* selectivity observed in **2c**+**A$_2$** is therefore the result of more severe reactant distortions that overwhelm the more favorable interaction energies in the *endo* TS. The geometries of reactants **2c** and **A$_2$** in their cycloaddition TS geometries provide an illustrative example of reactant distortions. (Table 2) The diene fragment is more heavily deformed at the *endo* TS by about 1.5 kcal/mol, and the dienophile is distorted twice as much, 3.1 kcal/mol. The origin of the dramatic difference in distortion energies of **A$_2$** in the two TSs is most easily visualized by a side-on view of the dienophile complex shown in Figure 5. The methyl group of dienophile **A$_2$** is bent out of the olefinic plane more severely in the *endo* TS (25°, Figure 5a) than in the *exo* TS (14°, Figure 5b), indicating that it suffers greater repulsion from the vicinal diene methyl in the *endo* TS.

A twist-asynchronous model shows how vicinal di-substitution can lead to a high distortion in the *endo* TS, which is chiefly responsible for the *exo* selectivity found computationally and experimentally.

In general, Diels–Alder reactions of unsymmetrical dienes and dienophiles proceed through concerted[43] asynchronous[44] mechanisms.[45] Two modes of asynchronicity in Diels–Alder reactions can be distinguished. (Figure 6) The stretch mode refers to the differing lengths of the two forming C–C bonds at the transition state. (Figure 6a) The twist mode refers to the deviation of the diene and the dienophile backbones from being parallel, and can be measured by a twist-asynchronicity parameter, θ, which is the C2−5−6−1 dihedral angle, where C5–C6 is the shorter forming C–C bond. (Figure 6b) The impact of catalyst coordination to stretch-mode asynchronicity of Diels–Alder reactions is well discussed.[46] A twist-asynchronous model was first put forward by Brown and Houk to account for substituent-induced selectivity variation in the context of intramolecular Diels–Alder (IMDA) reactions.[47] This has seen extensive application in the rationalization of stereoselectivity of the IMDA reactions of other substrates.[48]

Table 3 lists the *endo* and the *exo* TSs for the Diels–Alder reactions of a series of silyloxy dienes and other model dienes with the oxazolidinone-bearing dienophile **3**, either in the presence of Me$_2$AlCl (represented by the dienophile complex **A$_2$**) or in its absence. These are presented as Newman projections along the shorter forming (C5–C6) bond.

It is clear from Table 3 that the *endo* series of TSs displays a wider range of twist-mode asynchronicity than the *exo* TSs. Depending on diene substitution, θ varies from +12° to −33° for the *endo* TSs and from +10° to +23° for the *exo* TSs. The *endo* TS of the *exo*-selective **2c** +**A$_2$** cycloaddition is highly twisted, with $\theta = -33°$, and features a very small Me–Me dihedral angle of 23°. (Entry 1) The corresponding *exo* TS is much less twisted, and places the vicinal

Me groups at 72°. The wide difference in Me–Me dihedral angle in the two TSs explains why the dienophile complex experiences a higher distortion at the *endo* TS.

Replacing the C1-Me group on **2c** with hydrogen – resulting in the desmethyl diene **2e** – reduces the allylic 1,3-strain across the silyl enol ether and allows TSs containing the s-syn rotamer of **2e** to be located. These TSs are more stable than the corresponding TSs containing the s-anti conformer of **2e**, and are displayed in Entry 2. The levels of twisting are smaller, leading to similar H–Me dihedral angles in both TSs, concomitant with a much smaller relative stability of the *exo* TS. MP2 even predicts that the *endo* TS is more stable. The TS geometries and energies are therefore heavily affected by the C1-Me substituent in this system.

What causes the drastic asynchronous twist in the *endo* **2c**+$\mathbf{A_2}$ TS? To assess its origin, we modeled the TSs involving diene **2f**, in which a methoxy group replaces the silyloxy group in **2c** (Entry 3). The computed free energies of activation indicate that, as a result of this replacement, the *exo-endo* difference narrows down from 4.0 kcal/mol (Entry 1) to 2.3 kcal/mol (Entry 3). The *endo* TS is also less twisted, with $\theta = -13°$, placing the vicinal Me groups at a dihedral angle of 44°. The twist-asynchronicity and the resultant Me–Me dihedral angle are practically the same in the *exo* TSs involving either the methoxy or the silyloxy diene. Since the methoxy and the trimethylsilyloxy groups can be expected to possess similar electronic properties (both dominated by oxygen), steric interactions, plausibly between the trimethylsilyloxy group and the dimethylaluminum portion of $\mathbf{A_2}$, are one contributor to the high twist-asynchronicity in *endo* **2c**+$\mathbf{A_2}$ TS. Another destabilizing factor is electrostatic repulsion between the oxygenated group and the aluminum-bound dienophile. As the TSs of **2c**+**3** show, (Entry 4) the asynchronous twist is considerably less severe in the absence of Lewis acid, resulting in the more typical Me–Me dihedral angles of 67° (*endo*) and 75° (*exo*) respectively. The *exo* preference is again diminished; MP2 energies even indicate an *endo* preference. Electrostatic repulsion between the lone pair on a heterodienophile and the diene is well known to influence stereochemical preferences[49] and dictate reaction trajectories[50] of hetero-Diels–Alder reactions. Analogous interactions should also operate in the *endo* **2c**+$\mathbf{A_2}$ system.

Based on the discussion above, a twist-asynchronous model rationalizing substituent effects on relative *endo* and *exo* TS energies in the Diels–Alder reactions of silyloxydienes is presented in Figure 7. In the *endo* series of TSs (Figure 7a), steric and electrostatic interactions between the diene C2-substituent and the aluminum-complexed dienophile drives the rotation of the latter in the outward direction. This motion is disfavored when both ends of the shorter forming C5–C6 bond are methyl substituted, since the rotation brings them close together and aggravates vicinal repulsion between them. The twist-asynchronicity of these TSs reflects the tradeoff between the two types of repulsion arising from their respective local environments within the TSs. In contrast, the *exo* TSs are less prone to these destabilizing interactions. As Figure 7b shows, the twisting that would alleviate the steric and electrostatic interactions also brings any vicinal methyl substituents on the C5–C6 forming bond further apart. The *exo* series of TSs could therefore relax by asynchronous twisting as appropriate. Indeed, when the 2-silyloxy or 2-methoxydiene is methyl substituted at both of their termini, the *exo* TSs consistently displays a narrow range of Me–Me dihedral angle between 69° and 75°. (Table 3, Entries 1, 3 and 4) This model explains why the relative energies of the *endo* and the *exo* TS for a given cycloaddition depend heavily on the substitution pattern, and why the *exo* TSs are, in most cases, less destabilized than the *endo* TSs.

Computations of Diels–Alder TSs of the dienophile complex $\mathbf{A_2}$ with a series of structurally simpler dienes give further support to the twist-asynchronicity model. *Trans*-piperylene (**18**) was reported by Evans to react with **3*** in the presence of Et_2AlCl with an *endo/exo* selectivity superior to 95:5.[26] Modeling the TSs of the **18**+$\mathbf{A_2}$ addition (Table 3, Entry 5), with MP2

single-point energies, reproduced the experimental level and sense of the *endo*/*exo* selectivity. The twisting of these TSs is small and comparable to that of the TSs involving the 2-trimethylsilyloxydiene **2e** (Entry 2). The substituents around the shorter forming C–C bond are arranged in an approximately staggered manner. The low level of twisting of *endo* **18** +**A₂** TS could be favorably compared to that of the TSs computed in the dialkylaluminum chloride catalyzed Diels–Alder reaction of isoprene and acrolein. Singleton and Houk,[51] and Evanseck[52] have shown that the TSs of this reaction, which were validated by experimental and calculated kinetic isotope effects, correspond to the *endo* approach of the two reactants. These TSs display a low level of asynchronous twist and a nearly staggered arrangement of substituents around the shorter forming C–C bond, similar to the *endo* **18**+**A₂** TS. (Figure 8) Consequently, the greater stabilization of the *endo* transition states determine the stereoselectivity.

Adding a terminal methyl substituent to *trans*-piperylene gives 2,4-hexadiene **19**. *Exo* selectivity is now found (Table 3, Entry 6). In the *endo* TS, the backbones of the diene and the dienophile are skewed, with $\theta = +12°$. The Me–Me repulsion forces the dienophile away from ideal overlap with the remote terminus of the diene. Although the *endo* TS is now more destabilized (according to B3LYP energies), the magnitude of such destabilization is small (1.4 kcal/mol free energy difference) compared to the cases where the diene is additionally substituted at the 2-position. (2−4 kcal/mol, Table 3, Entries 1 and 3). The "back side" of the *endo* **19**+**A₂** TS is not hindered by substituents. This allows the dienophile to rotate inward to alleviate the vicinal dimethyl repulsion and the accompanying destabilization.

The phenyl substituted silylated dienes **1b** and **1a** used in the experimental studies were modeled by the methyl analogs **1d** and **1e** respectively. The free energies of activation of cycloadditions with **A₂** indicate that the *exo* preference is very high in the case of diene **1d** and much diminished for diene **1e**, where the C1-methyl group on the diene is replaced by hydrogen. (Figure 9) This trend is consistent with experimental results of the cycloadditions of **3*** with **1a** and with **1b** (Table 1, Entries 1−2). The moderate *endo* selectivity in the experimental **1a** +**3*** reaction could not be reproduced by B3LYP energies of the **1e**+**A₂** TSs, although MP2 single-points predict a much higher proportion of the *endo* product. MP2 methods have been shown, in some cases, to be more accurate in reproducing experimental trends, particularly when weak non-bonding interactions are involved.[5, 41, 53]

An analysis of distortion and interaction energies (Table 4) shows that the distortion energies in the *endo* TS again overwhelm the more favorable interaction energies in the presence of vicinal di-substitution, and account for the *exo* preference observed. The sum of distortion energies of the diene **1d** and dienophile complex **A₂** is 3.2 kcal/mol higher in the *endo* TS than in the *exo* TS, while the corresponding difference involving the desmethyl analog **1e** is only about 0.9 kcal/mol favoring the *endo* pathway.

Replacing the oxygen in **2c** and **2e** with methylene – giving respectively the all-carbon silylated dienes **1d** and **1e** – leads to considerable alleviation in twisting in both *endo* and *exo* TSs with **A₂**. (Table 5, Entries 1−2) These TSs display θ values between −6° and −15°. This is consistent with the reduction of electrostatic repulsion between the diene and dienophile fragments as a result of this replacement. To investigate the influence of the silyl functionality, we computed model TSs of reaction of **A₂** and 3-methylhexa-2,4-diene (**20**), in which the silyl group is replaced by a hydrogen. (Table 5, Entry 3) For the **20**+**A₂** addition, a difference in free energies of activation of 1.4 kcal/mol favoring the *exo* product was computed; this is the same in magnitude and direction as that involving the C2-desmethyl diene **19**, (Table 3, Entry 6) but is only half of that observed for the corresponding silylated diene **1d**. (Table 5, Entry 1) The C2-Me substituent on the diene does perturb the *endo* TS geometry, as the vicinal methyl groups are now set at a dihedral angle of 51°, compared to 71° in its absence. The change in the *exo*

TS geometry is negligible. An extra trimethylsilyl group on the diene, however, brings little perturbation on the geometries of either the *endo* or the *exo* TS in terms of twist-mode asynchronicity and vicinal Me–Me dihedral angles in **1d**+**A₂**. The amplified *exo* selectivity caused by the presence of the silyl group is likely to be electronic rather than steric in origin, although the precise underpinnings are more subtle in these cases.

Conclusion

A new series of substituent-dependent *exo*-selective Diels–Alder reactions involving silylated or silyloxy dienes and α,β-unsaturated N-acyloxazolidinone or ketone dienophiles has been studied experimentally and computationally. These reactions demonstrate the maximal stereochemical efficiency of the Diels–Alder reaction by installing four contiguous stereocenters in the cycloadduct with a very favorable *exo* selectivity and π-facial selectivity. A systematic experimental study identified the structural prerequisites in the starting materials for such a high level of *exo* preference, namely, simultaneous methyl substitution on the diene and dienophile termini involved in the shorter forming C–C bond. Based on computational investigations of both experimental and other model systems, a twist-mode asynchronicity model was put forward to understand the origin of *endo*/*exo* stereocontrol. Specifically, this work showed how the vicinal di-substituent effect could destabilize the highly asynchronous *endo* TSs, requiring rotations that reduce steric and electrostatic repulsion within the TSs at the expense of reactant distortion. Interaction energies favor the *endo* pathway, but this is overwhelmed by distortion that relieves gauche-type Me–Me repulsions. This work has moved us closer to a more comprehensive understanding of the factors controlling Diels–Alder *endo*/*exo* stereoselectivity. It should also contribute to more effective experimental planning in using this reaction in the stereodefined synthesis of many molecular targets featuring six-membered rings.

Supplementary Material

Refer to Web version on PubMed Central for supplementary material.

Acknowledgment

REFERENCES

1. Fringuelli, F.; Taticchi, A. The Diels–Alder Reaction: Selected Practical Methods. Wiley; Chichester: 2002.

2. Carey, FA.; Sundberg, RJ. Advanced Organic Chemistry, Part A: Structure and Mechanisms. Vol. 5 ed.. Springer; New York: 2007. p. 834-873.Kürti, L.; Czakó, B. Strategic Applications of Named Reactions in Organic Synthesis. Elsevier; 2005. p. 140-141.

3. Nicolaou KC, Snyder SA, Montagnon T, Vassilikogiannakis G. Angew. Chem. Int. Ed 2002;41:1668.

4. a Sammis GM, Flamme EM, Xie H, Ho DM, Sorensen EJ. J. Am. Chem. Soc 2005;127:8612. [PubMed: 15954764] b Pritchard RG, Stoodley RJ, Yuen W-H. Org. Biomol. Chem 2005;3:162. [PubMed: 15602612] c Pellegrinet SC, Spanevello RA. Org. Lett 2000;2:1073. [PubMed: 10804557] d Kozmin SA, Rawal VH. J. Org. Chem 1997;62:5252. e Fraile JM, García JI, Gracia D, Mayoral JA, Pires E. J. Org. Chem 1996;61:9479. f Node M, Nishide K, Imazato H, Kurosaki R, Inoue T, Ikariya T. Chem. Commun 1996:2559. g Ward DE, Gai Y. Tetrahedron Lett 1992;33:1851. h Lamy-Schelkens H, Giomi D, Ghosez L. Tetrahedron Lett 1989;30:5887. *Exo*-selective catalytic asymmetric Diels–Alder reactions of Danishefsky-type dienes and α,β-unsaturated N-acyloxazolidinones have also been

disclosed very recently: i Sudo Y, Shirasaki D, Harada S, Nishida A. J. Am. Chem. Soc 2008;130:12588. [PubMed: 18761458] For a report on an *exo*-selective Diels–Alder reaction that also includes a mechanistic discussion: j Ge M, Stoltz BM, Corey EJ. Org. Lett 2000;2:1927. [PubMed: 10891193]

5. Boren B, Hirschi JS, Reibenspies JH, Tallant MD, Singleton DA, Sulikowski GA. J. Org. Chem 2003;68:8991. [PubMed: 14604372]

6. a Cernak TA, Gleason JL. J. Org. Chem 2008;73:102. [PubMed: 18067312] b Qi J, Roush WR. Org. Lett 2006;8:2795. [PubMed: 16774259] c Roush WR, Barda DA, Limberakis C, Kunz RK. Tetrahedron 2002;58:6433. d Takeda K, Imaoka I, Yoshii E. Tetrahedron 1994;50:10839. e Pyne SG, Safaei-G J, Hockless DCR, Skelton BW, Sobolev AN, White AH. Tetrahedron 1994;50:941. f Roush WR, Brown BB. J. Org. Chem 1992;57:3380. g Adam W, Albert R, Hasemann L, Nava Salgado VO, Nestler B, Peters E-M, Peters K, Prechtl F, von Schnering HG. J. Org. Chem 1991;56:5782.

7. Corey EJ, Loh T-P. J. Am. Chem. Soc 1991;113:8966.

8. Yoon T, Danishefsky SJ, de Gala S. Angew. Chem. Int. Ed. Engl 1994;33:853.

9. Powers TS, Jiang W, Su J, Wulff WD, Waltermire BE, Rheingold AL. J. Am. Chem. Soc 1997;119:6438.

10. a Barluenga J, Canteli R-M, Flórez J, García-Granda S, Gutiérrez-Rodríguez A, Martín E. J. Am. Chem. Soc 1998;120:2514. b Richardson BM, Welker ME. J. Org. Chem 1997;62:1299. c Wright MW, Smalley TL, Welker ME, Rheingold AL. J. Am. Chem. Soc 1994;116:6777. d Sabat M, Reynolds KA, Finn MG. Organometallics 1994;13:2084. e Gilbertson SR, Zhao X, Dawson DP, Marshall KL. J. Am. Chem. Soc 1993;115:8517.

11. Maruoka K, Imoto H, Yamamoto H. J. Am. Chem. Soc 1994;116:12115.

12. Ahrendt KA, Borths CJ, MacMillan DWC. J. Am. Chem. Soc 2000;122:4243.

13. Ishihara K, Nakano K. J. Am. Chem. Soc 2005;127:10504. [PubMed: 16045334]

14. Kano T, Tanaka Y, Maruoka K. Org. Lett 2006;8:2687. [PubMed: 16774232]

15. Kano T, Tanaka Y, Maruoka K. Chem. Asian J 2007;2:1161. [PubMed: 17640000]

16. Gotoh H, Hayashi Y. Org. Lett 2007;9:2859. [PubMed: 17580885]

17. Walter CJ, Anderson HL, Sanders JKM. J. Chem. Soc., Chem. Commun 1993:458.

18. Pearson RJ, Kassianidis E, Philp D. Tetrahedron Lett 2004;45:4777.

19. a Cannizzaro CE, Ashley JA, Janda KD, Houk KN. J. Am. Chem. Soc 2003;125:2489. [PubMed: 12603137] b Heine A, Stura EA, Yli-Kauhaluoma JT, Gao C, Deng Q, Beno BR, Houk KN, Janda KD, Wilson IA. Science 1998;279:1934. [PubMed: 9506943] c Yli-Kauhaluoma JT, Ashley JA, Lo C-H, Tucker L, Wolfe MM, Janda KD. J. Am. Chem. Soc 1995;117:7041. d Gouverneur VE, Houk KN, de Pascual-Teresa B, Beno B, Janda KD, Lerner RA. Science 1993;262:204. [PubMed: 8211138]

20. Lam, Y.-h.; Bobbio, C.; Cooper, IR.; Gouverneur, V. Angew. Chem. Int. Ed 2007;46:5106.

21. For related Diels–Alder reactions of all-carbon silylated dienes, see: a Ryu DH, Corey EJ. J. Am. Chem. Soc 2003;125:6388. [PubMed: 12785777] b Vedejs E, Duncan SM. J. Org. Chem 2000;65:6073. [PubMed: 10987942] c Organ MG, Winkle DD. J. Org. Chem 1997;62:1881. d Corey EJ, Letavic MA. J. Am. Chem. Soc 1995;117:9616. e Krafft GA, Garcia EA, Guram A, O'Shaughnessy B, Xu X. Tetrahedron Lett 1986;27:2691. f Sakurai H, Hosomi A, Saito M, Sasaki K, Iguchi H, Sasaki J-I, Araki Y. Tetrahedron 1983;39:883. g Trost BM, Shimizu M. J. Am. Chem. Soc 1982;104:4299. h Ojima I, Yatabe M, Fuchikami T. J. Org. Chem 1982;47:2051.

22. a Frankowski KJ, Golden JE, Zeng Y, Lei Y, Aubé J. J. Am. Chem. Soc 2008;130:6018. [PubMed: 18396881] b Alonso D, Caballero E, Medarde M, Tomé F. Tetrahedron Lett 2007;48:907. c Caballero E, Alonso D, Peláez R, Álvarez C, Puebla P, Sanz F, Medarde M, Tomé F. Tetrahedron 2005;61:6871. d Caballero E, Alonso D, Peláez R, Alvarez C, Puebla P, Sanz F, Medarde M, Tomé F. Tetrahedron Lett 2004;45:1631.

23. a Nakashima D, Yamamoto H. J. Am. Chem. Soc 2006;128:9626. [PubMed: 16866505] b Ruijter E, Schültingkemper H, Wessjohann LA. J. Org. Chem 2005;70:2820. [PubMed: 15787578] c Boezio AA, Jarvo ER, Lawrence BM, Jacobsen EN. Angew. Chem. Int. Ed 2005;44:6046. d Chaplin JH, Edwards AJ, Flynn BL. Org. Biomol. Chem 2003;1:1842. [PubMed: 12945762] e Kraus GA, Hon YS, Sy J, Raggon J. J. Org. Chem 1988;53:1397. f Bell VL, Holmes AB, Hsu S-Y, Mock GA, Raphael RA. J. Chem. Soc., Perkin Trans 1986;1:1507.

24. a Narayanan BA, Bunnelle WH. Tetrahedron Lett 1987;28:6261. b Hayashi T, Katsuro Y, Kumada M. Tetrahedron Lett 1980;21:3915. c Yamamoto Y, Yamamoto H. Angew. Chem. Int. Ed 2005;44:7082. d Kanemasa S, Kumegawa M, Wada E, Nomura M. Bull. Chem. Soc. Jpn 1991;64:2990. See also refs. [20] and [23a].

25. a Evans DA, Chapman KT, Bisaha J. J. Am. Chem. Soc 1984;106:4261. b Thom C, Kocienski P. Synthesis 1992:582. c Kanemasa S, Kanai T. J. Am. Chem. Soc 2000;122:10710.

26. Evans DA, Chapman KT, Bisaha J. J. Am. Chem. Soc 1988;110:1238.

27. For a recent example of the use of this chiral auxiliary in an *exo*-selective asymmetric hetero Diels–Alder reaction: Evans DA, Scheidt KA, Downey CW. Org. Lett 2001;3:3009. [PubMed: 11554830]

28. a Zeng Y, Aubé J. J. Am. Chem. Soc 2005;127:15712. [PubMed: 16277507] b Zeng Y, Reddy DS, Hirt E, Aubé J. Org. Lett 2004;6:4993. [PubMed: 15606118]

29. Armstrong A, Davies NGM, Martin NG, Rutherford AP. Tetrahedron Lett 2003;44:3915.

30. a Becke AD. J. Chem. Phys 1993;98:1372. b Becke AD. J. Chem. Phys 1993;98:5648. c Lee C, Yang W, Parr RG. Phys. Rev. B 1988;37:785.

31. a Hehre WJ, Ditchfield R, Pople JA. J. Chem. Phys 1972;56:2257. b Hariharan PC, Pople JA. Theor. Chim. Acta 1973;28:213.

32. Tomasi J, Persico M. Chem. Rev 1994;94:2027.

33. Takano Y, Houk KN. J. Chem. Theory Comput 2005;1:70.

34. Birney DM, Houk KN. J. Am. Chem. Soc 1990;112:4127.

35. Frisch, MJ., et al. Gaussian 03. Gaussian, Inc.; Wallingford, CT: 2004. Rev. C.02 & D.01

36. Castellino S, Dwight WJ. J. Am. Chem. Soc 1993;115:2986.

37. Bickelhaupt FM. J. Comput. Chem 1999;20:114.

38. DeChancie J, Acevedo O, Evanseck JD. J. Am. Chem. Soc 2004;126:6043. [PubMed: 15137769]

39. Nagase S, Morokuma K. J. Am. Chem. Soc 1978;100:1666.

40. a Ess DH, Houk KN. J. Am. Chem. Soc 2008;130:10187. [PubMed: 18613669] b Ess DH, Houk KN. J. Am. Chem. Soc 2007;129:10646. [PubMed: 17685614] c Ess DH, Jones GO, Houk KN. Org. Lett 2008;10:1633. [PubMed: 18363405] d García JI, Martínez-Merino V, Mayoral JA, Salvatella L. J. Am. Chem. Soc 1998;120:2415. e Sbai A, Branchadell V, Ortuño RM, Oliva A. J. Org. Chem 1997;62:3049. [PubMed: 11671684]

41. Wannere CS, Paul A, Herges R, Houk KN, Schaefer HF III, Schleyer P. v. R. J. Comput. Chem 2007;28:344. [PubMed: 17109435]

42. Tsuzuki S, Lüthi HP. J. Chem. Phys 2001;114:3949.

43. a Goldstein E, Beno B, Houk KN. J. Am. Chem. Soc 1996;118:6036. b Storer JW, Raimondi L, Houk KN. J. Am. Chem. Soc 1994;116:9675. c Houk KN, Lin YT, Brown FK. J. Am. Chem. Soc 1986;108:554.

44. a Singleton DA, Schulmeier BE, Hang C, Thomas AA, Leung S-W, Merrigan SR. Tetrahedron 2001;57:5149. b Beno BR, Houk KN, Singleton DA. J. Am. Chem. Soc 1996;118:9984.

45. Houk KN, Gonzalez J, Li Y. Acc. Chem. Res 1995;28:81. For an up-to-date discussion of Diels–Alder mechanisms, see also: BachrachSMComputational Organic Chemistry2007128-133John Wiley & Sons, Inc.

46. García JI, Mayoral JA, Salvatella L. J. Am. Chem. Soc 1996;118:11680. See also refs [34, 40d, and 40e].

47. a Brown FK, Houk KN. Tetrahedron Lett 1985;26:2297. b Wu T-C, Houk KN. Tetrahedron Lett 1985;26:2293.

48. a Tripoli R, Cayzer TN, Willis AC, Sherburn MS, Paddon-Row MN. Org. Biomol. Chem 2007;5:2606. [PubMed: 18019536] b Paddon-Row MN, Moran D, Jones GA, Sherburn MS. J. Org. Chem 2005;70:10841. [PubMed: 16356007] c Cayzer TN, Paddon-Row MN, Moran D, Payne AD, Sherburn MS, Turner P. J. Org. Chem 2005;70:5561. [PubMed: 15989338] d Lilly MJ, Paddon-Row MN, Sherburn MS, Turner CI. Chem. Commun 2000:2213.

49. Iafe RG, Houk KN. J. Org. Chem 2008;73:2679. [PubMed: 18327949]

50. a Leach AG, Houk KN. J. Org. Chem 2001;66:5192. [PubMed: 11463273] b McCarrick MA, Wu YD, Houk KN. J. Org. Chem 1993;58:3330.

51. Singleton DA, Merrigan SR, Beno BR, Houk KN. Tetrahedron Lett 1999;40:5817.

52. Acevedo O, Evanseck JD. Org. Lett 2003;5:649. [PubMed: 12605481]

53. a Dinadayalane TC, Vijaya R, Smitha A, Sastry GN. J. Phys. Chem. A 2002;106:1627. b Baki S, Maddaluno J, Derdour A, Chaquin P. Eur. J. Org. Chem 2008:3200. c Bakalova SM, Santos AG. J. Org. Chem 2004;69:8475. [PubMed: 15549823] d Bakalova SM, Kaneti J. J. Phys. Chem. A. ASAP, DOI: 10.1021/jp803701y
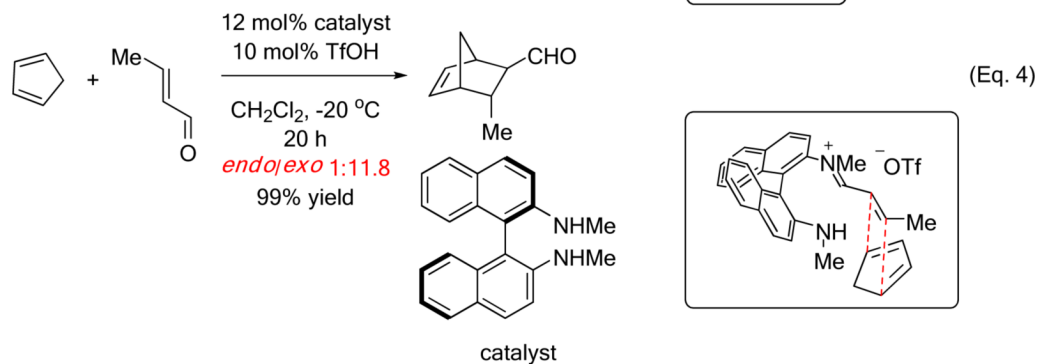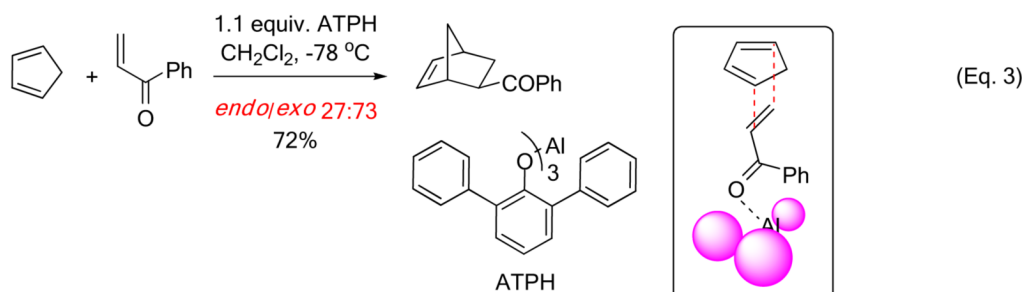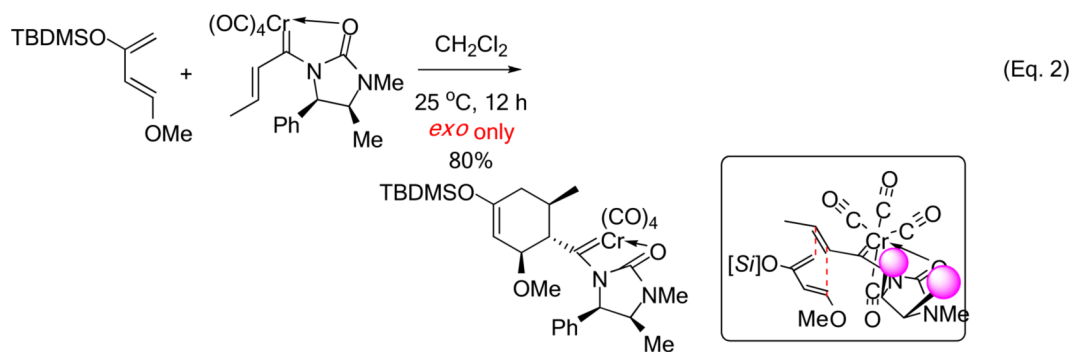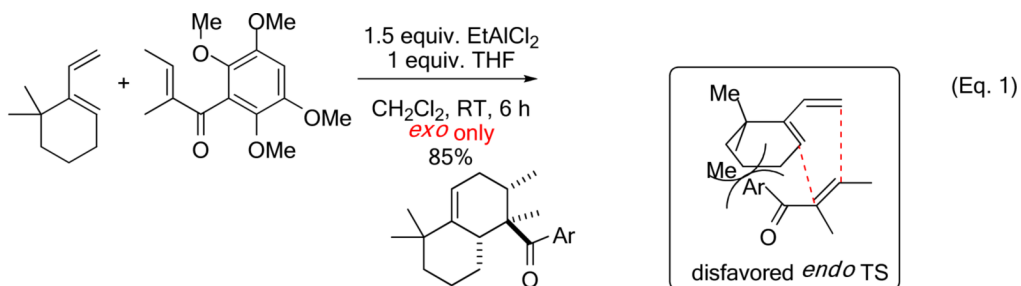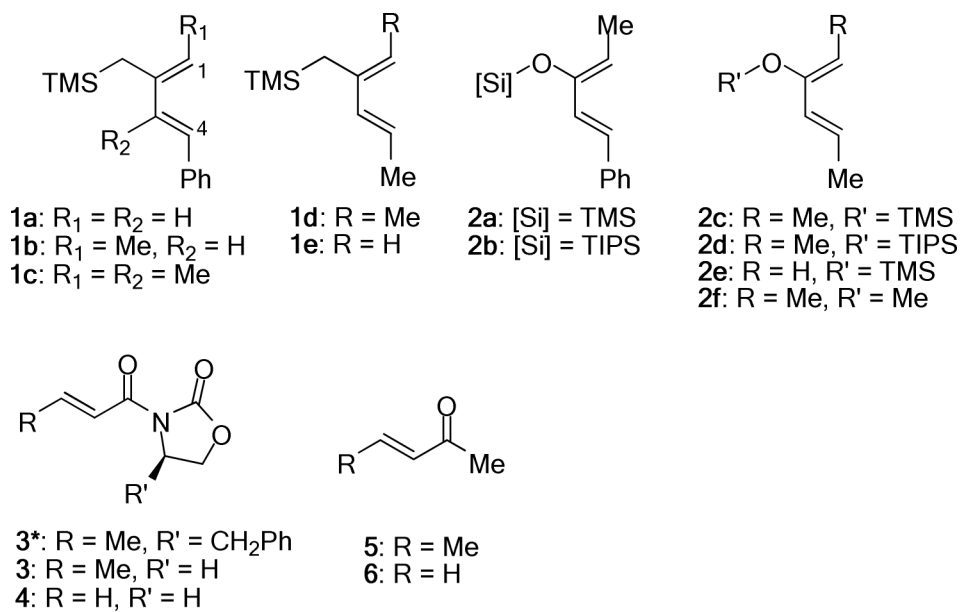
Scheme 1.
Selected Examples of Substrate- and Catalyst-Controlled *Exo*-Selective Intermolecular Diels–Alder Reactions.
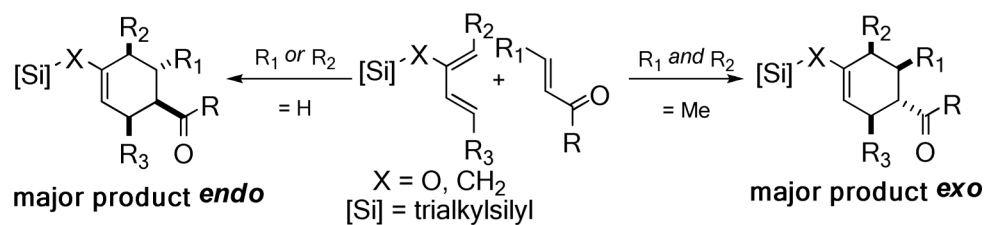
Scheme 2.
Stereochemical Dependence on Substitution Pattern of Starting Materials.

1a: R$_1$ = R$_2$ = H
1b: R$_1$ = Me, R$_2$ = H
1c: R$_1$ = R$_2$ = Me

1d: R = Me
1e: R = H

2a: [Si] = TMS
2b: [Si] = TIPS

2c: R = Me, R' = TMS
2d: R = Me, R' = TIPS
2e: R = H, R' = TMS
2f: R = Me, R' = Me

3*: R = Me, R' = CH$_2$Ph
3: R = Me, R' = H
4: R = H, R' = H

5: R = Me
6: R = H

Chart 1.
Structure of Dienes **1−2** and Dienophiles **3−6**.
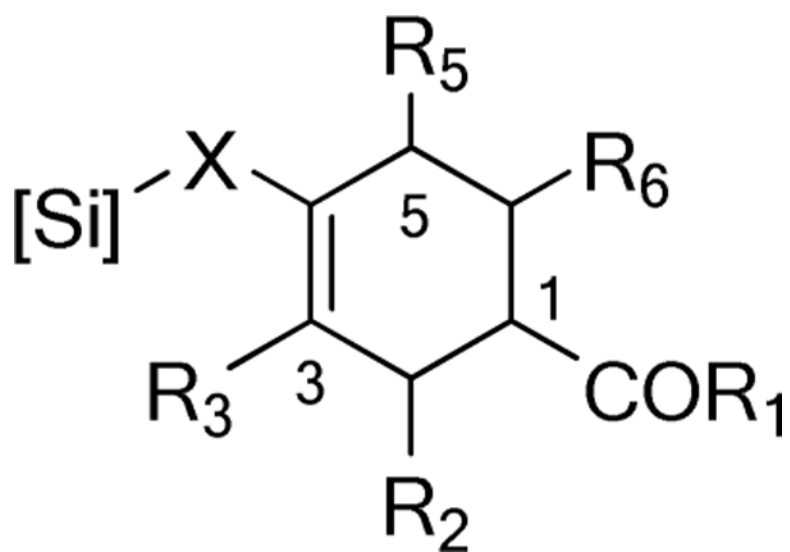
Figure 1.
Numbering of Cycloadducts.
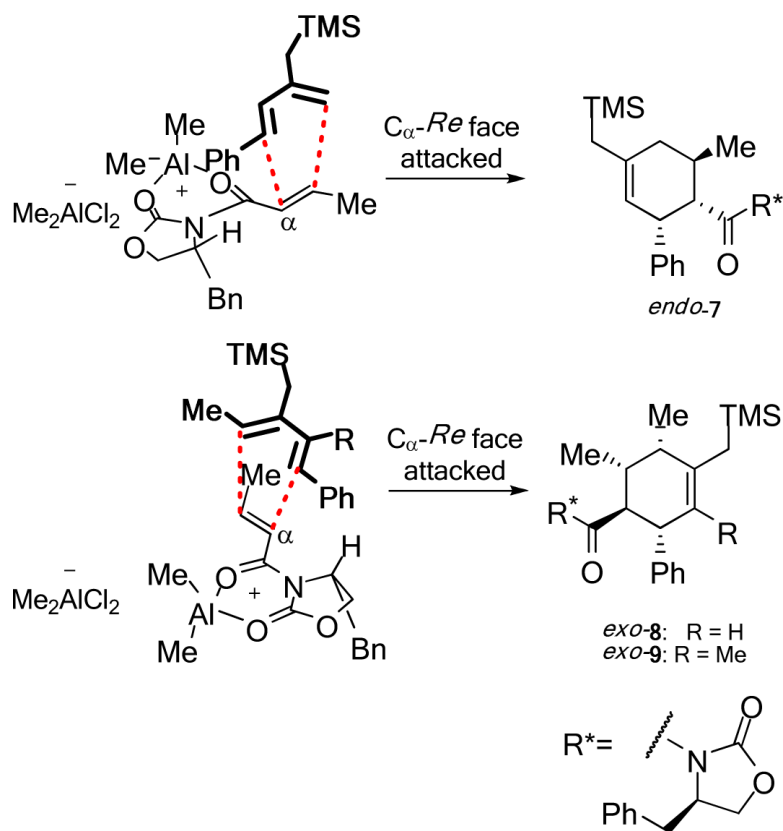
Figure 2.
Rationalization of the Sense of Asymmetric Induction in the **1a–1c** + **3*** Cycloadditions.
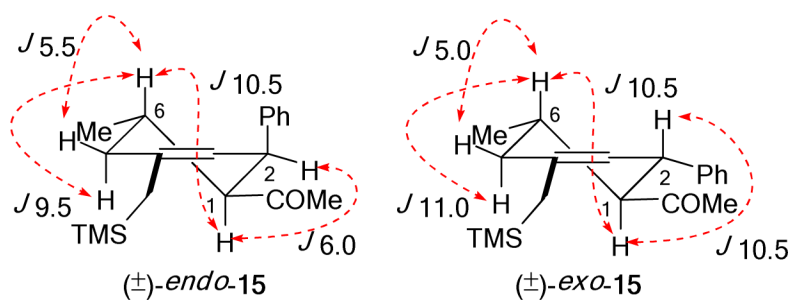
Figure 3.
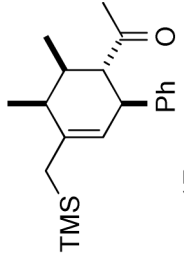Key NMR Coupling Constants for Stereochemical Assignments Illustrated for *Endo*- and *Exo*-**15**.
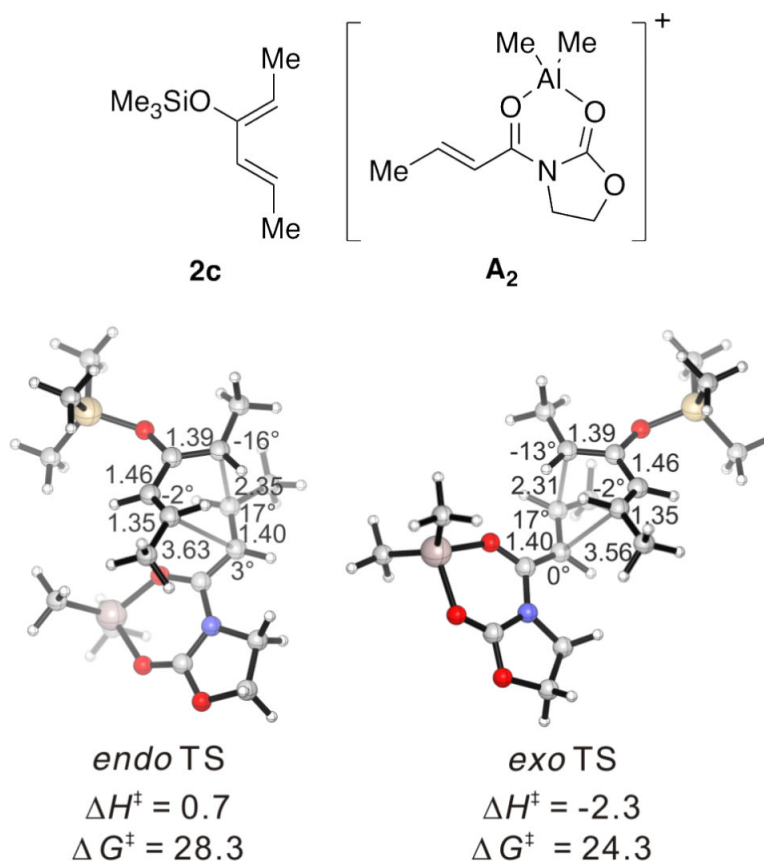
Figure 4.
Endo and *Exo* TSs of the **2c**+**A$_2$** Cycloadditions. Gas-phase enthalpies of activation computed at the B3LYP/6−31G(d) level. Free energies of activation computed by B3LYP/6−31G(d), corrected for solvent effects by PCM single-points at HF/6−31+G(d,p). Interatomic distances around the forming ring in Å and angles of pyramidalization at the termini of the partially formed bonds are labeled.
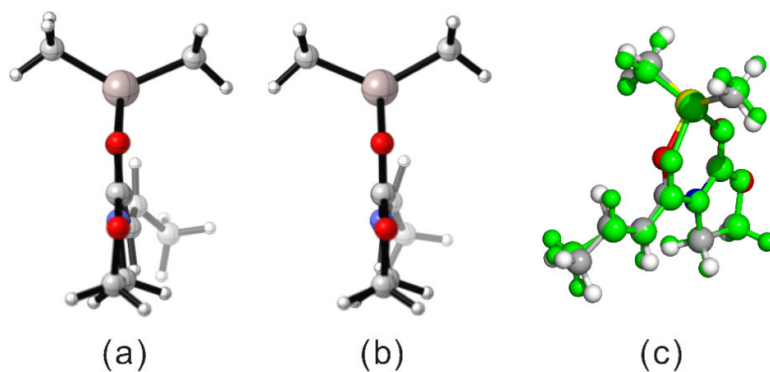
Figure 5.
Side View of A_2 Dienophile Fragment in (a) the *Endo* **2c**+A_2 TS, and (b) the *Exo* **2c**+A_2 TS. (c) Overlay of A_2 Dienophile Fragments in TSs of **2c**+A_2 (Green: *Endo*, Other-Colored Atoms: *exo*).
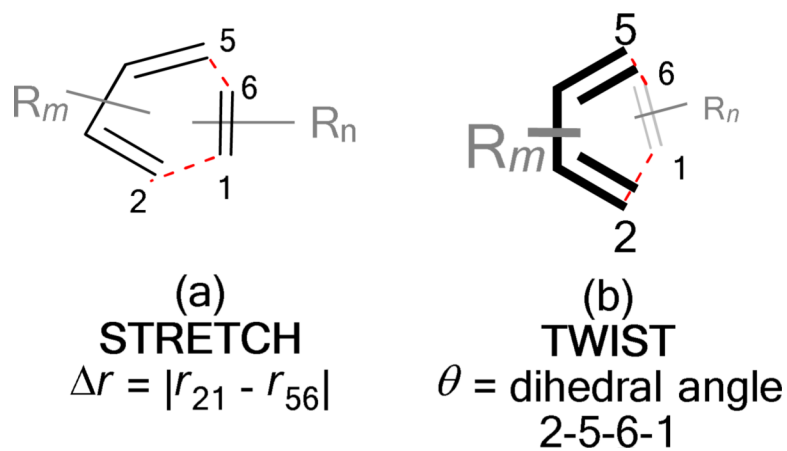
Figure 6.
Schematic Illustration of the Two Modes of Asynchronicity at the Transition State of a Diels–Alder Reaction.
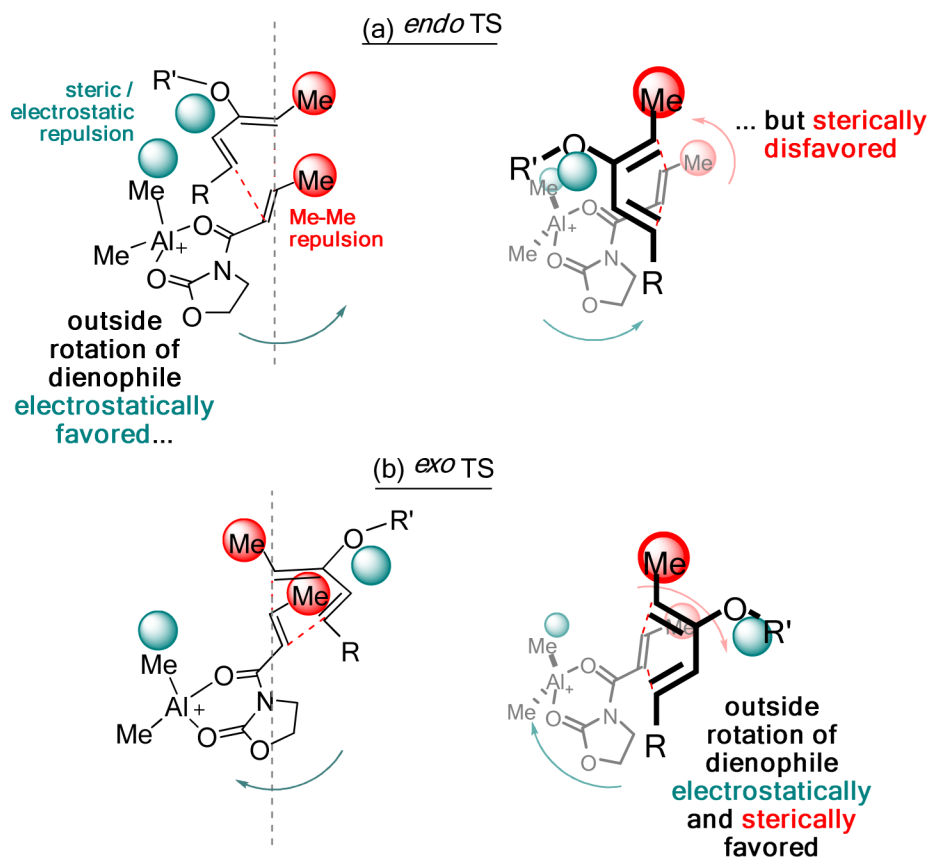
Figure 7.
A Twist-Asynchronicity Model Delineating the Origin of *Exo* Selectivity in Diels–Alder Reactions Involving Oxygenated Dienes.
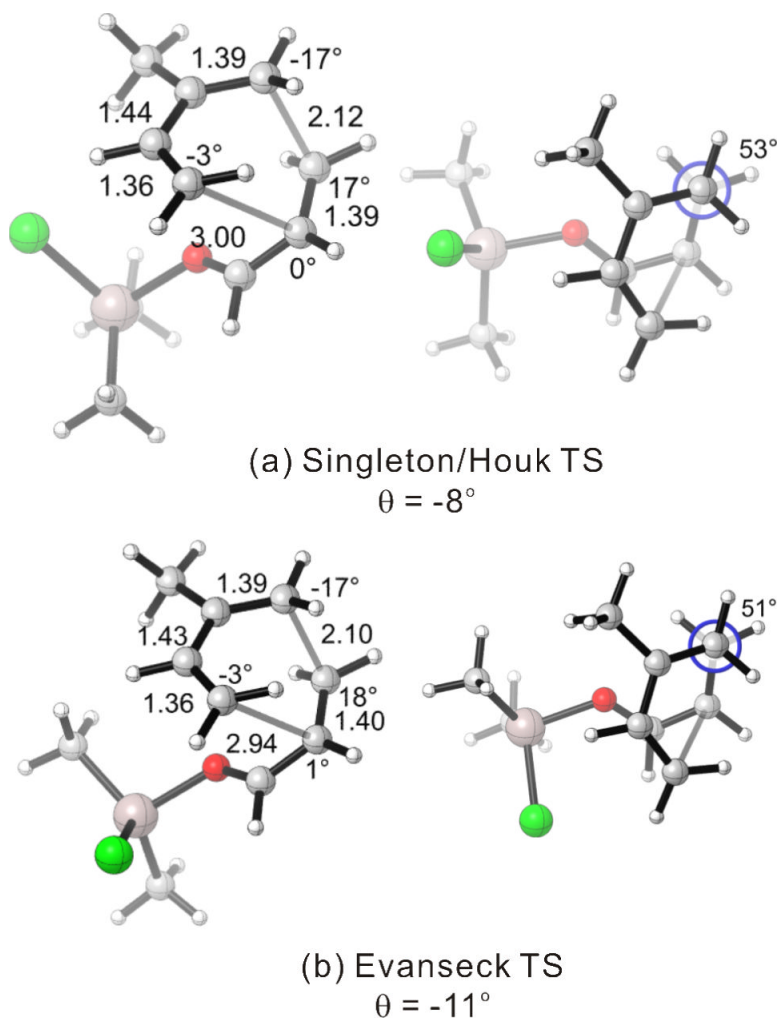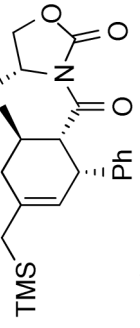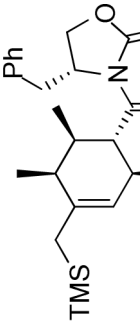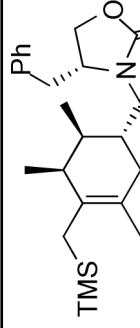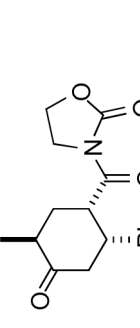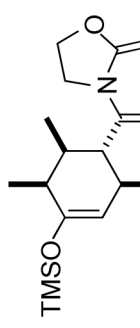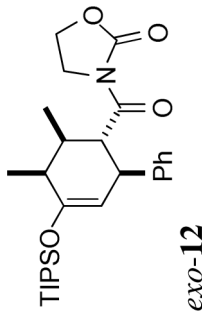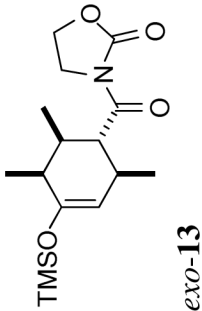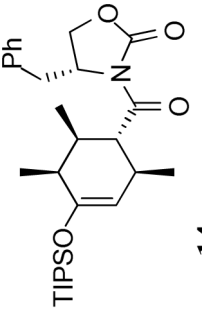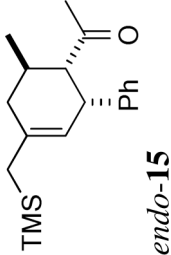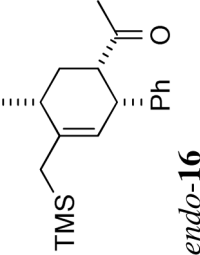
Figure 8.
The B3LYP/6−31G(d) *Endo* TSs for the Reaction of Isoprene with Acrolein•AlMe$_2$Cl Obtained by Singleton/Houk and Evanseck.
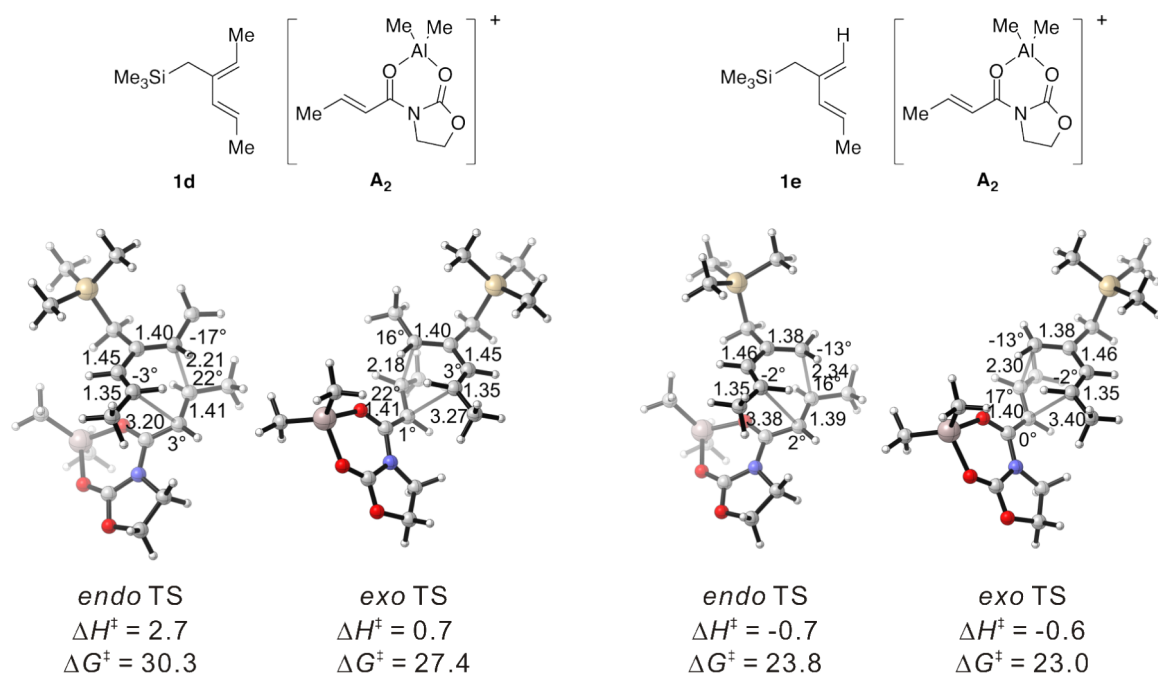
Figure 9.
Endo and *Exo* TSs of the **1d** and **1e**+**A₂** Cycloadditions. Gas-phase enthalpies of activation computed at the B3LYP/6−31G(d) level. Free energies of activation computed by B3LYP/6 −31G(d), corrected for solvent effects by PCM single-points at HF/6−31+G(d,p). Interatomic distances around the forming ring in Å and angles of pyramidalization at the termini of the partially formed bonds are labeled.

Table 1

Intermolecular Diels–Alder Reactions Involving Oxazolidinone Dienophiles.

Entry	Reacting partners	Conditions	Major product	exo/endo[a]	Yield
1[b]	1a + 3*	1.4 equiv. Me$_2$AlCl, CH$_2$Cl$_2$, –40 °C	endo-7	1:5	50%
2[c]	1b + 3*		exo-8	> 20:1	58%
3[d]	1c + 3*		exo-9	> 20:1	65%
4[e]	2a + 4		endo-10[f]	1:20	78%
5	2a + 3		exo-11	> 20:1	62%

Entry	Reacting partners	Conditions	Major product	exo/endo[a]	Yield
6	2b + 3		exo-**12**	> 20:1	89%
7	2c + 3		exo-**13**	> 20:1	80%
8	2d + 3*	0.2–0.3 equiv. Me$_2$AlCl, CH$_2$Cl$_2$, RT	exo-**14**	> 20:1	48%
9	1a + 5		endo-**15**	1:4	15% exo 62% endo
10[c]	1b + 6		endo-**16**	1:10	4% exo 40% endo

Entry	Reacting partners	Conditions	Major product	exo/endo[a]	Yield
11[c]	1b + 5		*exo*-**17**	11: (1:1.5:0.4)[g]	78% *exo*

[a] By 400 MHz ^{1}H NMR of the product mixture after aqueous workup.

[b] ref. 20.

[c] **1b** used as an inseparable isomeric mixture with (Z,E):(E,E) = 3:1. Reaction of only the major isomer was observed unless otherwise stated.

[d] **1c** used as a mixture with (Z,E):(E,E) = 5:1. Only reaction from the major isomer was observed.

[e] At −100 °C.

[f] Product of protodesilylation of the primary, *endo* cycloadduct, epimerized at C5, was isolated after chromatographic purification over silica gel.

[g] Four sets of signals were observed by ^{1}H NMR of the crude mixture. Two of the adducts were assigned as *exo*-**17** and its C-5 epimer. The other two, minor adducts were tentatively assigned as the corresponding *endo* isomers.
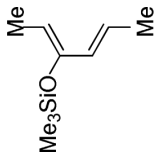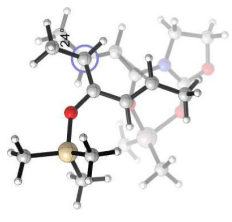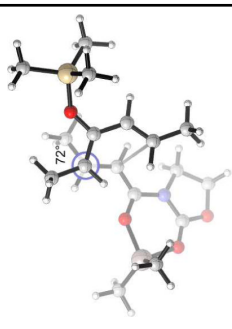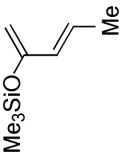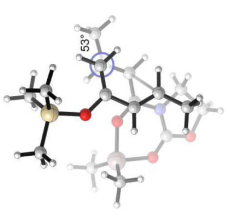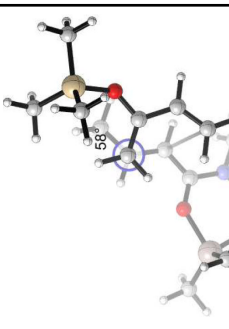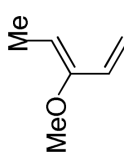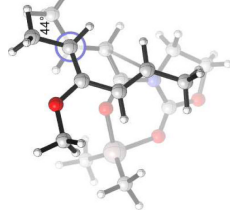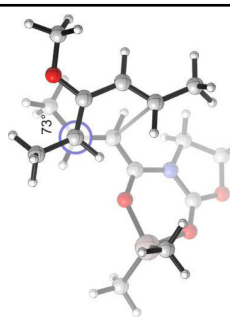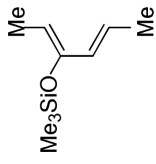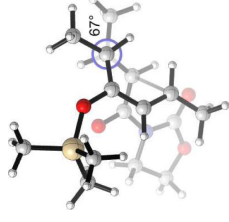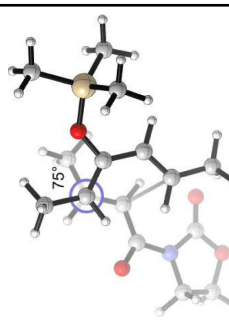
Table 2

Activation Barriers and Their Dissection into Distortion and Interaction Energies for *Endo* and *Exo* TSs of **2c**+**A**$_2$ (kcal/mol).

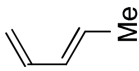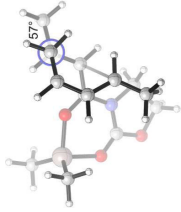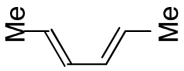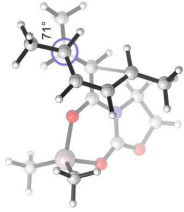| Entries	Method		$\Delta E^{\ddagger}$	$\Delta E_d^{\ddagger}$		$\Delta E_i^{\ddagger}$
				diene **2c**	dienophile complex **A**$_2$	
1	B3LYP/6−31G(d)	*endo*	−0.1	9.5	11.9	−21.4
2		*exo*	−3.0	7.9	8.8	−19.7
3	MP2/6−31+G(d)	*endo*	−11.4	9.8	12.0	−33.1
4		*exo*	−13.5	8.3	8.8	−30.6

Table 3

Endo (n) and *Exo* (x) TS Geometries and Energetics for a Range of Silyloxydienes and Other Model Dienes with Dienophile Complex **A₂** or Dienophile **3**, with an Emphasis on Twist-Mode Asynchronicity.

Entry	Diene	TS geometry		$\Delta G^{\ddagger}_{298}$ [a]	$\Delta E_0^{\ddagger b}$	θ^c	Me(H)–Me dihedral angle
		endo	*exo*				
1	2c			28.3(n) 24.3(x)	−0.1 (−11.4) (n) −3.0 (−13.5) (x)	−33° (n) +22° (x)	24°(n) 72°(x)
2	2e			24.1(n) 24.0(x)	−2.0 (−13.1) (n) −2.1 (−11.4) (x)	−5°(n) +10°(x)	53°(n) 58°(x)
3	2f			25.9(n) 23.6(x)	0.4 (−11.0) (n) −1.7 (−11.4) (x)	−13°(n) +23°(x)	44°(n) 73°(x)
4[d]	2c			42.7(n) 40.1 (x)	21.0 (4.5) (n) 20.2 (5.6) (x)	+9°(n) +23°(x)	67°(n) 75°(x)

Entry	Diene	TS geometry	$\Delta G^{\ddagger}_{298}$ [a]	$\Delta E^{\ddagger}_{0}$ [b]	θ [c]	Me(H)–Me dihedral angle
5	Me **18**		28.9(n) 29.6(x)	6.9 (−3.8) (n) 7.3 (−2.1) (x)	−3°(n) +12°(x)	57°(n) 58°(x)
6	Me Me **19**		34.7(n) 33.3(x)	10.6 (−4.2) (n) 9.1 (−4.5) (x)	+12°(n) +16°(x)	71°(n) 64°(x)

[a] Gas phase Gibbs energy at B3LYP/6−31G(d) level, corrected for solvent effects by PCM single-points at HF/6−31+G(d,p) on B3LYP/6−31G(d) vacuum optimized geometries.

[b] Gas phase uncorrected electronic energy at B3LYP/6−31G(d)//B3LYP/6−31G(d) level. The corresponding energy at MP2/6−31+G(d)//B3LYP/6−31G(d) level in parentheses.

[c] Twist-asynchronicity parameter. See Figure 6b for definition.

[d] In the absence of Me2AlCl (i.e. with dienophile **3**).

Table 4

Activation Barriers and Their Dissection into Distortion and Interaction Energies for *Endo* and *Exo* TSs of **1d and 1e+A$_2$** (kcal/mol).

Entries	Reactants	Method		$\Delta E^{\ddagger}$	$\Delta E_d^{\ddagger}$		$\Delta E_i^{\ddagger}$
					diene	dienophile complex A$_2$	
1	1d+A$_2$	B3LYP/6–31G(d)	endo	2.0	10.9	14.2	−23.2
2			exo	−0.1	9.2	12.7	−22.0
3		MP2/6–31+G(d)	endo	−14.8	10.0	14.3	−39.1
4			exo	−14.1	8.4	12.7	−35.2
5	1e+A$_2$	B3LYP/6–31G(d)	endo	−1.4	6.0	7.6	−15.0
6			exo	−1.3	6.3	8.2	−15.8
7		MP2/6–31+G(d)	endo	−12.9	5.9	7.6	−26.3
8			exo	−11.2	6.1	8.2	−25.4

Table 5

Endo (n) and *Exo* (x) TS Geometries and Energetics for a Range of Substituted Silylated Dienes with Dienophile Complex **A$_2$**, with an Emphasis on Twist-Mode Asynchronicity.

Entry	Diene	TS geometry		$\Delta G^{\ddagger}_{298}$ [a]	$\Delta E_0^{\ddagger}$ [b]	θ [c]	Me(H)–Me dihedral angle
		endo	*exo*				
1	Me$_3$Si ... Me **1d**	47°	69°	30.3(n) 27.4(x)	2.0 (−14.8) (n) −0.1 (−14.1) (x)	−6°(n) +15°(x)	47°(n) 69°(x)
2	Me$_3$Si ... Me **1e**	52°	57°	23.8(n) 23.0(x)	−1.4 (−12.9) (n) −1.3 (−11.2) (x)	−6°(n) +8°(x)	52°(n) 57°(x)
3	Me ... Me **20**	51°	66°	31.3(n) 29.9(x)	6.8 (−9.8) (n) 5.5 (−9.4) (x)	−4°(n) +13°(x)	51°(n) 66°(x)

[a] Gas phase Gibbs energies at B3LYP/6–31G(d) level, corrected for solvent effects by PCM single-points at HF/6–31+G(d,p) on B3LYP/6–31G(d) vacuum optimized geometries.

[b] Gas phase uncorrected electronic energy at B3LYP/6–31G(d)//B3LYP/6–31G(d) level. The corresponding MP2/6–31+G(d)//B3LYP/6–31G(d) level in parentheses.

[c] Twist-asynchronicity parameter. See Figure 6b for definition.